Analysis of βB1-crystallin unfolding equilibrium by spin and fluorescence labeling: Evidence of a dimeric intermediate

Hanane A. Koteiche, M. Satish Kumar, Hassane S. Mchaourab*

Department of Molecular Physiology and Biophysics, Vanderbilt University, Nashville, TN 37232, USA

Abstract **A central step in understanding lens aging is to characterize the thermodynamic stability of its proteins and determine the consequences of changes in the primary sequence on their folding equilibria. For this purpose, destabilized mutations were introduced in βB1-crystallin targeting the domain interface within the fold of a subunit. Global unfolding was monitored by tryptophan fluorescence while concomitant structural changes at the dimer interface were monitored by fluorescence and spin labels. Both spectral probes report explicit evidence of multi-state unfolding equilibrium. The biphasic nature of the unfolding curves was more pronounced at higher protein concentration. Distinct shifts in the midpoint of the second transition reflect the population of a dimeric intermediate. This intermediate may be a critical determinant for the life-long stability of the β-crystallins and has important consequences on interactions with α-crystallin.**
© 2007 Federation of European Biochemical Societies. Published by Elsevier B.V. All rights reserved.

1. Introduction

The optical properties of the vertebrate lens are a consequence of a complex interplay between stability, solubility and interaction of proteins [1,2]. The central players in this molecular environment are three classes of proteins, the α-, β- and γ-crystallins [2]. As the lens ages without turnover of its fiber cells and their protein constituents, the crystallins accumulate post-translational modifications such as truncations, oxidations and modifications of side chains [1]. These events are bound to alter the free energies of folding, solubility and protein–protein interactions. In the most common disease state of the lens, age-related cataract, crystallin aggregates accumulate and disrupt protein packing leading to loss of transparency.

There are seven β-crystallins in the human lens that assemble in vivo into an array of homo- and hetero-oligomers [3]. βB1-crystallin undergoes age-related modifications that reduce its stability [4,5]. Because βB1-crystallin is the building block of a native mixed oligomer, changes in its stability may have significant impact on protein organization in the fiber cells. In solution, recombinant βB1- and βB2-crystallins behave as dimers over a range of concentrations while γ-crystallins are monomers despite similar domain and secondary structure organizations.

A potential attractive force between crystallins is a consequence of the affinity of α-crystallin, the lens resident chaperone, to destabilized proteins [6]. Co-aggregation of crystallins is more prevalent in aged and cataractous lenses suggesting that the various modifications of β- and γ-crystallins enhance their interactions with α-crystallin [7]. The simplest thermodynamic model of α-crystallin interaction with its substrates links the apparent affinity to the substrate free energy of unfolding [8]. Previous work from our laboratory focused on the model substrate T4 Lysozyme (T4L) with a two-state unfolding equilibrium. Extension of these studies to the native substrates, the β- and γ-crystallins, requires a thorough characterization of their folding equilibria.

Denaturant unfolding of β- and γ-crystallins has generally been interpreted in terms of a three-state model [3,9]. Indirect evidence of the population of an intermediate included the broad shape of the unfolding transitions and in the case of βB2-crystallin the dependence of stability on protein concentration [10]. More recent studies of mutants of βB2-crystallin reported explicit detection of three-state unfolding transitions [11,12].

The βB2-crystallin dimer is stabilized by intermolecular packing of the N- and C-terminal domains of the two symmetry-related subunits [13]. The folding intermediate was proposed to be monomeric with an unfolded N-terminus [10]. Despite extensive sequence similarity, the crystal structure of truncated βB1-crystallin reveals intramolecular packing of the two domains resulting in a subunit fold similar to that of the monomeric γ-crystallin [14]. The dimer contact surface resembles that formed between dimers of βB2-crystallin in the crystal lattice [14]. Thus, it is not clear whether the folding model of βB2- applies to βB1-crystallin.

This report explores the consequences of the different dimerization motifs on the stability [15] of βB1-crystallin using tryptophan fluorescence in conjunction with spin and fluorescence labeling. Unfolding curves of destabilizing mutations uncover intermediate states whose apparent stabilities display explicit dependence on protein concentration. The multi-state nature of βB1-crystallin unfolding has important consequences on its effective affinity and mode of interaction with α-crystallin [15].

*Corresponding author.
E-mail address:* hassane.mchaourab@vanderbilt.edu (H.S. Mchaourab).

2. Materials and methods

2.1. Protein expression, purification and labeling

Human βB1-crystallin cloned into the pET3a vector was a generous gift from Dr. Christine Slingsby. Site-directed mutagenesis was performed as previously described [12]. Protein expression was carried out using the auto-induction method for 14 h at 30 °C [16]. After cell lysis and DNA precipitation, βB1-crystallin was purified by anion exchange chromatography [12]. The purified protein was then reacted with a 10-fold molar excess of either spin label I or bimane label and allowed to incubate for 2 h at room temperature (Scheme 1). The reaction mixture was then purified by size-exclusion chromatography on a Superdex 75 column in buffer containing 15 mM (Tris/Mes), 50 mM NaCl, pH 7.2. The bimane labeled mutants are referenced with the suffix B$_2$; the spin labeled mutants with the suffix R1. The bimane labeling efficiency was determined by comparing the absorption at 280 nm and 380 nm.

2.2. Conformational stability of βB1 mutants

The conformational stability of βB1-crystallin mutants at 37 °C, pH 7.2 was determined by denaturant-unfolding tryptophan fluorescence on a PTI L-format spectrofluorometer. βB1-crystallin solutions at constant concentrations were titrated with increasing guanidine hydrochloride (GdmHCl) concentration. The unfolding curves were obtained by plotting the emission intensity ratio at two wavelengths, 320 nm and 350 nm, as a function of GdmHCl concentration. The excitation wavelength was 295 nm. Unless otherwise indicated, all curves were collected at 2 μM βB1-crystallin concentration. Where appropriate, the unfolding curves were analyzed by the method of Grimsley et al. [17].

2.3. Fluorescence spectroscopy

Fluorescence emission spectra of bimane-labeled samples were recorded between 400 nm and 500 nm after exciting the bimane molecule at 380 nm.

2.4. EPR spectroscopy

Electron paramagnetic resonance (EPR) spectra were collected on a Bruker EMX spectrometer using a super high Q resonator. The microwave power was 5 mW and the modulation amplitude 1.6 G.

3. Results and discussion

3.1. Design of the mutants

The mutations, previously selected to destabilize the dimer interface of βB2-crystallin structure [12], map to the domain interface within the tertiary fold of a βB1-crystallin monomer
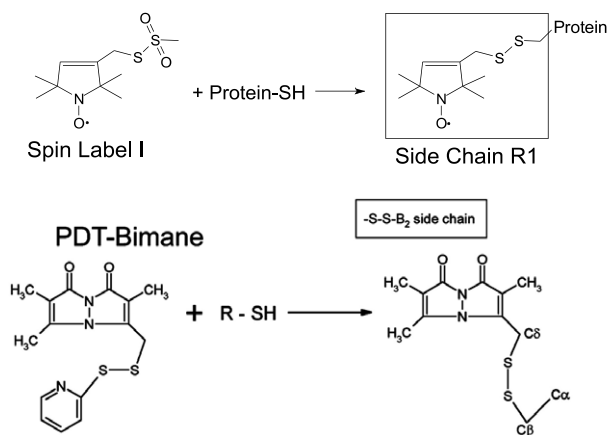
Scheme 1.

(Fig. 1). L206A reduces the buried surface areas while E208L disrupts an electrostatic interaction with R139 without significant changes in the steric volume of the side chain.

To monitor local structural changes, spin or bimane labels were attached at cysteine 79 of βB1-crystallin located in a surface loop or at a cysteine introduced at position 117 at the dimer interface in a background where C79 was replaced with a valine (C79V). At site 79, the probes monitor the N-terminal domain in a subunit while at site 117 they monitor the dimer interface. Analysis of the labeled and unlabeled mutants by far-UV CD reveals little change in the content of secondary structure compared to the unlabeled wild type (WT) (data not shown).

3.2. Stable intermediates in βB1-crystallin equilibrium unfolding

The equilibrium unfolding of βB1-crystallin and its destabilized mutants was investigated by monitoring parallel changes in tryptophan (trp) and bimane fluorescences. The substitutions result in a left shift of the trp unfolding curves consistent with a reduction in the thermodynamic stability of the folded state. Fig. 2A shows that attachment of the bimane probe also contributes to the loss of stability despite the location of the native cysteine 79 in a solvent-exposed loop. In general, the transitions are broad and less cooperative than expected for a two-state equilibrium consistent with the population of intermediate states. For all mutants in the WT background, hereafter referred to as C79, the unfolding was essentially reversible as illustrated in Fig. 2A.

Fig. 2B shows that the L206A substitution exposes the population of an intermediate state manifested by a pronounced plateau in the trp unfolding curve. Two distinct transitions,
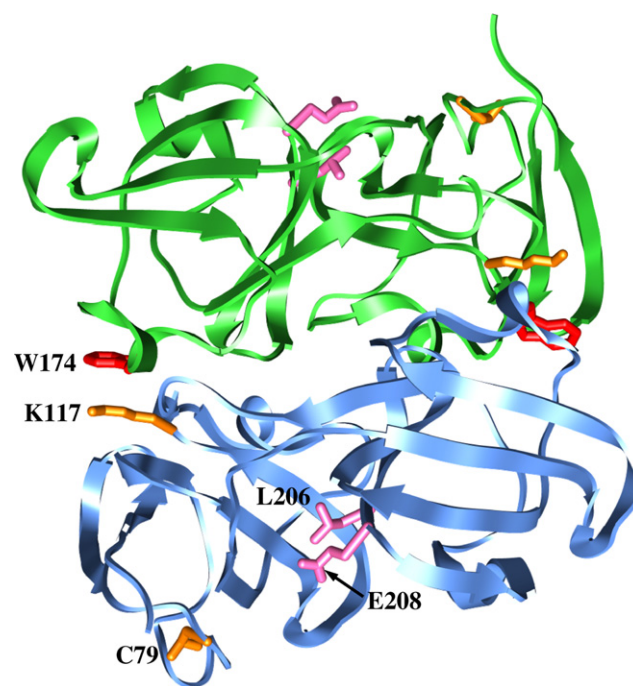

Fig. 1. Ribbon representation of βB1-crystallin crystal structure showing the sites of destabilizing mutations (pink), the sites of probe attachment (orange) and trp 174 (red). The two subunits in the crystallographic dimer are shown in cyan and green.
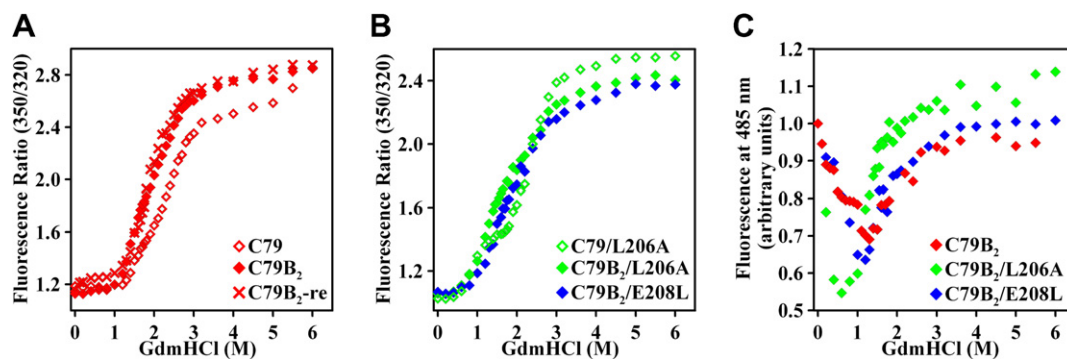
Fig. 2. (A) and (B) trp unfolding curves of βB1-crystallin demonstrating the destabilization induced by bimane labeling and the L206A and E208L substitutions. (C) Biphasic bimane unfolding curves explicitly reveal the population of an intermediate state. Open and closed symbols are used for unlabeled and labeled βB1-crystallin, respectively; re refers to equilibrium refolding from 6 M GdmHCl.

representative of a three-state equilibrium, can be gleaned: a transition from the folded state to an intermediate between 0 and 2 M GdmHCl and a transition from the intermediate to the unfolded state between 2 and 3 M GdmHCl. Compared to C79, the left shift occurs in the early part of the curves suggesting a reduction in the stability of the native state relative to a folding intermediate. In contrast, subsequent bimane labeling of L206A shifts the second part of the curve implying a destabilization of the intermediate relative to the unfolded state.

In the absence of a direct manifestation of the unfolding intermediate, quantitative analysis of these curves is hindered by the large number of parameters to be determined (data not shown). Nevertheless, the stability ranking of the mutants, derived qualitatively from comparing the GdmHCl concentrations at the curves midpoint, is not unexpected given the more drastic nature of the L206A substitution.

The bimane unfolding curves provide direct evidence for the population of an intermediate (Fig. 2C). For all three mutants, a distinct change in the bimane intensity occurs at low GdmHCl concentration where no changes in the trp fluorescence are reported. The left shift in the dip position indicates a destabilization of the folded state relative to the intermediate as a consequence of the mutations. Further increase in GdmHCl concentration resets the intensity to that of the folded state. Because the cysteine attachment site of the bi-

mane is in a loop, global unfolding is not expected to significantly affect the bimane properties. Such trends at loop sites were also observed for unfolding of bimane-labeled T4L (Claxton and Mchaourab, unpublished results).

3.3. The dimer interface in the unfolding intermediate

The current model of βB2-crystallin unfolding envisions a monomeric intermediate with an unfolded N-terminus. To probe whether βB1-crystallin populates such an intermediate, the bimane was introduced at site K117 at the dimer interface in close proximity to W174 in the C79V background. The tryptophan quenches the bimane fluorescence in the native dimer and provides a sensor of the packing of this interface during unfolding [18].

Fig. 3A shows that the cysteine substitution and the subsequent bimane labeling reduce the overall stability of the native state. Comparison with unlabeled K117C shows a distinct change in shape in the range of GdmHCl concentrations (2–3 M) that corresponds to the transition from the intermediate to the unfolded state.

In the K117C background, the trp unfolding curves of L206A and to a lesser extent E208L are biphasic indicating the population of a stable intermediate (Fig. 3B). Attachment of the bimane label leads to a left shift in the transitions to lower GdmHCl concentrations. Comparison of Figs. 3B and Fig. 4A reveals that the shift occurs in the part of the unfolding
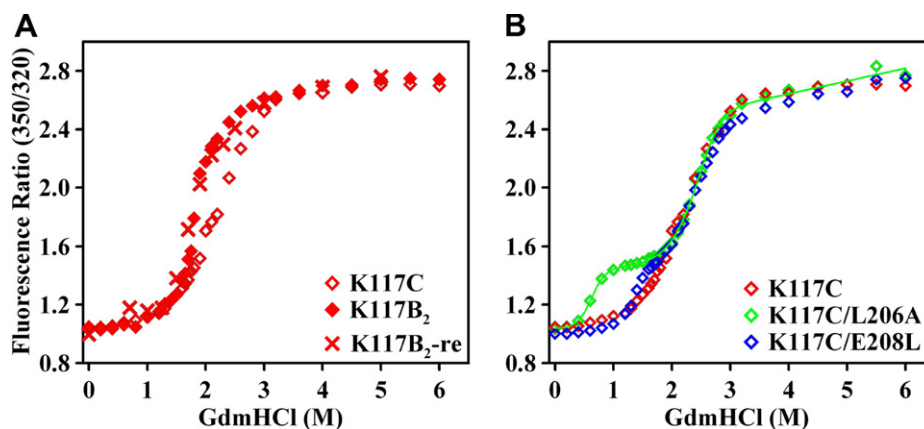

Fig. 3. Trp unfolding curves of βB1-crystallin and its variants in the C79V/K117C background. Open and closed symbols are used for unlabeled and labeled βB1-crystallin; re refers to equilibrium refolding from 6 M GdmHCl. The solid line is a non-linear least-squares fit using the parameters in Table 1.
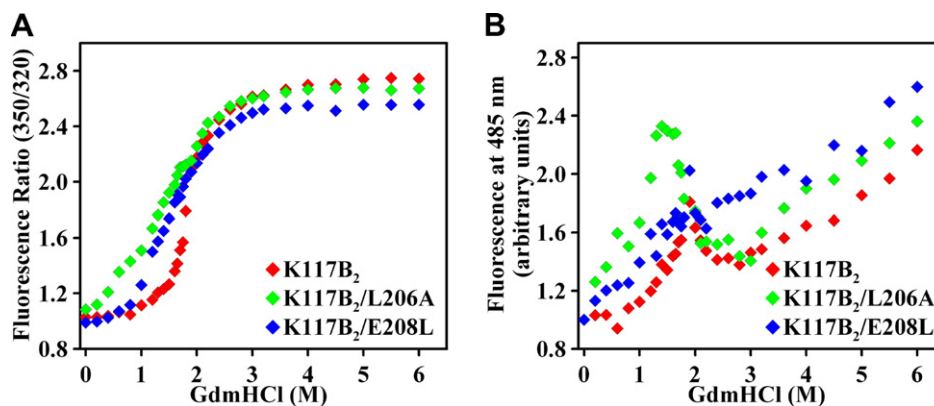
Fig. 4. (A) trp and (B) bimane unfolding curves of βB1-crystallin labeled at site K117. The y axis in panel B has been normalized relative to the emission intensity in the absence of GdmHCl.
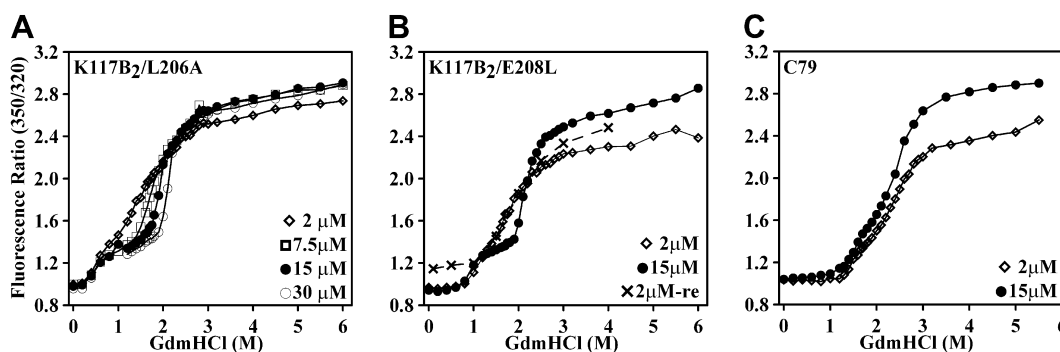

Fig. 5. Dependence of βB1-crystallin equilibrium unfolding on protein concentration. (A) K117B$_2$/L206A, (B) K117B$_2$/E208L, and (C) C79. re refers to equilibrium refolding from 6 M GdmHCl.

curve corresponding to the transition from the intermediate to the unfolded state. Given that the cysteine substitution at K117 and subsequent labeling weakens contacts at the dimer interface, these results are consistent with the preservation of the interface in the intermediate.

The multi-state nature of unfolding is manifested by the biphasic change in bimane intensity as a function of GdmHCl concentration (Fig. 4B). Global unfolding of the mutants at 6 M GdmHCl induces an increase in the emission intensity of the bimane reflecting the dissociation of the dimer and the consequent separation of the bimane/trp pair. Signal enhancement at lower concentrations suggests rearrangements at the dimer interface in the intermediate.

Two features of the bimane unfolding curves in the K117C background suggest that this intermediate is distinct from that detected in Fig. 2C. First, the change in the bimane emission occurs at higher GdmHCl concentrations than in the C79 background despite the fact that mutants in the K117C background are less stable based on the trp unfolding curves (Figs. 2B and Fig. 4A). Second, the curves cannot be fit with a three-state model unless the intensity of the bimane emission in the intermediate is assumed to be larger than in the unfolded state.

3.4. A dimeric intermediate in the unfolding equilibrium of βB1-crystallin

If the intermediate is a dimer then its unfolding is coupled to dissociation. The coupling will be manifested by a dependence of the unfolding curves on protein concentration [17]. Fig. 5A

shows that the unfolding curves for K117B$_2$/L206A display an explicit dependence on protein concentration. The curves are almost superimposable in the low range of GdmHCl concentrations that corresponds to the transition from the native state to the intermediate while a clear shift is observed in the midpoint of the second transition. The concentration dependence is also observed for K117B$_2$/E208L but is less pronounced for the unlabeled C79 (Fig. 5B and C).

Unlike the mutants in the C79 background, the unfolding curves are not fully reversible in the range of GdmHCl that corresponds to the transition between the intermediate and the folded state. We verified by size-exclusion chromatography that at concentrations between 2 and 15 μM the labeled mutants do not aggregate in the presence of 1 M GdmHCl (data not shown). Table 1 reports the values of the free energies associated with the two transitions. It is clear that the coupled dimer dissociation and unfolding requires a large energy input and in fact accounts for the remarkable stability of this protein.

3.5. EPR analysis of βB1-crystallin unfolding

We used spin labeling and EPR spectroscopy to further characterize the structure of βB1-crystallin intermediates. Unfolded states lead invariably to a characteristic, highly mobile spin label lineshape that reflects backbone flexibility at the site of attachment [19]. Such spectrum was observed at GdmHCl concentrations corresponding to the unfolding plateau in the trp or bimane curves (Fig. 6). Spectral lineshapes at intermediate

Table 1
Free energy, ΔG, and m, the denaturant dependence of ΔG, for the two transitions of βB1-crystallin unfolding

βB1-crystallin	$D \rightleftharpoons I$		$I \rightleftharpoons 2U$	
	ΔG (kcal/mol)	m (kcal/mol M^{-1})	ΔG_{un}(kcal/mol)	m (kcal/mol M^{-1})
C79/L206A (2 μM)	4.4 ± 1.7	5.4 ± 2	16 ± 0.6	3.2 ± 0.3
K117C/L206A (2 μM)	3.1 ± 1.3	5 ±1.5	17.5 ± 0.8	3.8 ± 0.3
K117B$_2$/L206A (15 μM)	2.3 ± 0.3	4 ± 1.3	17.3 ± 1.1	5 ± 0.5

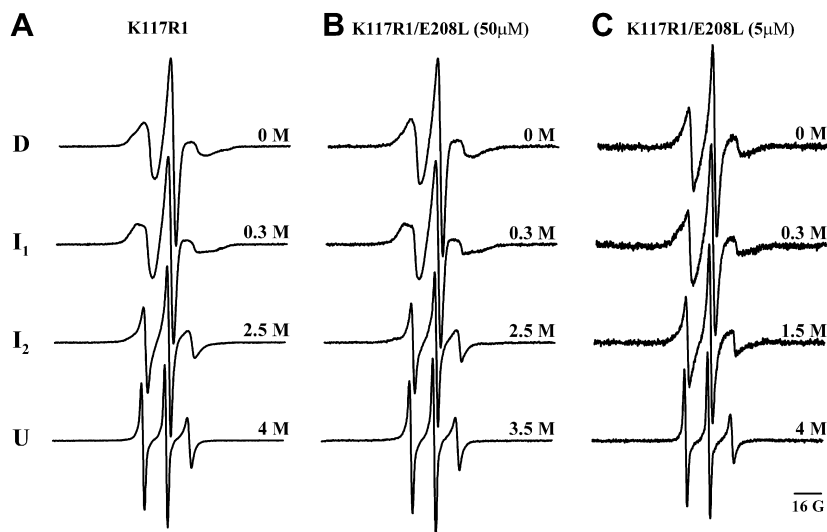The analysis used the formalism of Grimsley et al. [17].

Fig. 6. Detection of equilibrium intermediates by spin labeling EPR. (A) K117R1, (B) and (C) K117R1/E208L.

denaturant concentrations identify two motional states consistent with the population of two intermediates. Increasing GdmHCl to 0.3 M increases the ordering of the spin label relative to the native state (D) suggesting local structural rearrangements. At GdmHCl concentrations that populate the intermediate in the bimane unfolding curves, the mobility increases although to a lesser extent than the unfolded state.

The spin label mobility also uncovers a change in the structural dynamic of the E208L mutant as a function of protein concentration. The spectral lineshape at low concentration is indicative of a more flexible structure (Fig. 6B and C). Further analysis can be carried out by moving the spin labels to different locations.

4. Concluding remarks

The simplest model consistent with our data is a multi-state equilibrium that includes two intermediates in addition to the native dimer and unfolded states:

$$D \rightleftharpoons I_1 \rightleftharpoons I_2 \rightleftharpoons 2U \qquad (1)$$

The explicit concentration dependence of the stability of I_2 indicates that it is a dimer although with substantial rearrangements at the interface.

The apparent increase in the stability of βB1-crystallin at higher concentrations likely plays a critical role in buffering the effects of age-related damage and thus in the long-term stability of these proteins. Furthermore, it should reduce the tendency to associate with α-crystallin thereby delaying the titration of the chaperone capacity in the lens.

References

[1] Bloemendal, H., de Jong, W., Jaenicke, R., Lubsen, N.H., Slingsby, C. and Tardieu, A. (2004) Ageing and vision: structure, stability and function of lens crystallins. Prog. Biophys. Mol. Biol. 86, 407–485.
[2] Wistow, G.J. and Piatigorsky, J. (1988) Lens crystallins: the evolution and expression of proteins for a highly specialized tissue. Ann. Rev. Biochem. 57, 479–504.
[3] Jaenicke, R. and Slingsby, C. (2001) Lens crystallins and their microbial homologs: structure, stability and function. Crit. Rev. Biochem. Mol. Biol. 36, 435–499.
[4] David, L.L., Azuma, M. and Shearer, T.R. (1994) Cataract and the acceleration of calpain-induced β-crystallin insolubilization occurring during normal maturation of rat lens. Investig. Ophthalmol. Vis. Sci. 35, 785–793.
[5] Lampi, K.J., Oxford, J.T., Bachinger, H.P., Shearer, T.R., David, L.L. and Kapfer, D.M. (2001) Deamidation of human βB1 alters the elongated structure of the dimer. Exp. Eye Res. 72, 279–288.
[6] Horwitz, J. (2003) Alpha-crystallin. Exp. Eye Res. 76, 145–153.
[7] Truscott, R.J.W. (2005) Age-related nuclear cataract-oxidation is the key. Exp. Eye Res. 80, 709–725.
[8] Sathish, H.A., Stein, R.A., Yang, G. and Mchaourab, H.S. (2003) Mechanism of chaperone function in small heat-shock proteins. Fluorescence studies of the conformations of T4 lysozyme bound to αB-crystallin. J. Biol. Chem. 278, 44214–44221.

[9] Flaugh, S.L., Mills, I.A. and King, J. (2006) Glutamine deamidation destabilizes human γD-crystallin and lowers the kinetic barrier to unfolding. J. Biol. Chem. 281, 30782–30793.

[10] Wieligmann, K., Mayr, E.M. and Jaenicke, R. (1999) Folding and self-assembly of the domains of βB2-crystallin from rat eye lens. J. Mol. Biol. 286, 989–994.

[11] Lampi, K.J., Amyx, K.K., Ahmann, P. and Steel, E.A. (2006) Deamidation in human lens βB2-crystallin destabilizes the dimer. Biochemistry 45, 3146–3153.

[12] Sathish, H.A., Koteiche, H.A. and Mchaourab, H.S. (2004) Binding of destabilized βB2-crystallin mutants to α-crystallin: the role of a folding intermediate. J. Biol. Chem. 279, 16425–16432.

[13] Slingsby, C. and Clout, N.J. (1999) Structure of the crystallins. Eye 13, 395–402.

[14] Van Montfort, R.L.M., Bateman, O.A., Lubsen, N.H. and Slingsby, C. (2003) Crystal structure of truncated human βB1-crystallin. Protein Sci. 12, 2606–2612.

[15] Mchaourab, H.S., Koteiche, H.A. and Kumar, M.S. (2007) Specificity of αA-crystallin binding to destabilized mutants of βB1-crystallin. FEBS Lett., this issue, doi:10.1016/j.febslet.2007.04.005.

[16] Studier, F.W. (2005) Protein production by auto-induction in high density shaking cultures. Protein Express. Purif. 41, 207–234.

[17] Grimsley, J.K., Scholtz, J.M., Pace, C.N. and Wild, J.R. (1997) Organophosphorus hydrolase is a remarkably stable enzyme that unfolds through a homodimeric intermediate. Biochemistry 36, 14366–14374.

[18] Mansoor, S.E., Mchaourab, H.S. and Farrens, D.L. (2002) Mapping proximity within proteins using fluorescence spectroscopy. A study of T4 lysozyme showing that tryptophan residues quench bimane fluorescence. Biochemistry 41, 2475–2484.

[19] Hubbell, W.L., Mchaourab, H.S., Altenbach, C. and Lietzow, M.A. (1996) Watching proteins move using site-directed spin labeling. Structure 4, 779–783.